Salt Enhances Disease Resistance and Suppresses Cell Death in Ceramide Kinase Mutants[1][OPEN]

Yu-Bing Yang, Jian Yin, Li-Qun Huang, Jian Li, Ding-Kang Chen, and Nan Yao[2,3]

State Key Laboratory of Biocontrol, Guangdong Provincial Key Laboratory of Plant Resources, School of Life Sciences, Sun Yat-sen University, Guangzhou 510275, P. R. China

ORCID ID: 0000-0002-2045-5462 (N.Y.).

Sphingolipids act as structural components of cellular membranes and as signals in a variety of plant developmental processes and defense responses, including programmed cell death. Recent studies have uncovered an interplay between abiotic or biotic stress and programmed cell death. In a previous study, we characterized an Arabidopsis (*Arabidopsis thaliana*) cell-death mutant, *accelerated cell death5* (*acd5*), which accumulates ceramides and exhibits spontaneous cell death late in development. In this work, we report that salt (NaCl) treatment inhibits cell death in the *acd5* mutant and prevents the accumulation of sphingolipids. Exogenous application of abscisic acid (ABA) and the salicylic acid (SA) analog benzothiadiazole demonstrated that the effect of NaCl was partly dependent on the antagonistic interaction between endogenous SA and ABA. However, the use of mutants deficient in the ABA pathway suggested that the intact ABA pathway may not be required for this effect. Furthermore, pretreatment with salt enhanced the resistance response to biotic stress, and this enhanced resistance did not involve the pathogen-associated molecular pattern-triggered immune response. Taken together, our findings indicate that salt inhibits sphingolipid accumulation and cell death in *acd5* mutants partly via a mechanism that depends on SA and ABA antagonistic interaction, and enhances disease resistance independent of pattern-triggered immune responses.

Plants sense and respond to environmental conditions rapidly through a series of signal transmission and transduction processes. Moreover, when plants confront repeated stresses, the previous stressor may shape the plant's response to subsequent stresses. More specifically, pretreatment with an abiotic stress could prime the plant's response to biotic stresses. For example, pretreatment with salt can protect Arabidopsis (*Arabidopsis thaliana*) from pathogen infection through priming of pathogen-associated molecular pattern-triggered immunity (PTI; Singh et al., 2014).

Salinity is a substantial stressor, causing imbalances in ion homeostasis, cellular energy supplies, and redox conditions (Huh et al., 2002; Baena-González et al., 2007). Salt stress can cause an increase in electrolyte leakage, which results from dysfunction of the plasma membrane and ion accumulation (Verslues et al., 2006; Ben Rejeb et al., 2015). When plants encounter salt stress, their physiological states change to acclimate to the growth conditions; for example, some plants accumulate Pro, which may stabilize cellular homeostasis.

When plants experience high-salinity conditions, the abscisic acid (ABA) pathway is induced to adjust the plant's metabolism to cope with the stress (Raghavendra et al., 2010). In response to abiotic stresses (salinity, drought, cold), ABA biosynthesis and signaling are activated to regulate stomatal movement, ion channels, and hydrogen peroxide (H_2O_2) levels for maintaining water levels and balancing ion homeostasis (Raghavendra et al., 2010). In response to biotic stresses, ABA regulates the closing of stomata, which are natural entrances for pathogens. Melotto et al. (2006) demonstrated that pathogenic bacteria can take advantage of ABA signaling to promote opening of the stomata and thus ensure successful invasion.

The well-studied de novo ABA biosynthesis pathway starts from carotenoids and many important genes have been identified in this pathway (Nambara and Marion-Poll, 2005). In the ABA biosynthesis pathway, salt (NaCl) treatment strongly induces expression of the gene encoding 9-cis-epoxycarotenoid dioxygenase (NCED3), which cleaves neoxanthin and violaxanthin into xanthoxin (Iuchi et al., 2001; Barrero et al., 2006). Furthermore, ABA has an antagonistic interaction with the salicylic acid (SA) pathway by affecting SA

[1]This work was supported by the National Natural Science Foundation of China (31570255; 31771357; and 31700221), the Natural Science Foundation of Guangdong Province (2017A030311005), Fundamental Research Funds for the Central Universities (18lgpy51), and the China Postdoctoral Science Foundation (2016M592575).

[2]Author for contact: yaonan@mail.sysu.edu.cn.

[3]Senior author.

The author responsible for distribution of materials integral to the findings presented in this article in accordance with the policy described in the Instructions for Authors (www.plantphysiol.org) is: Nan Yao (yaonan@mail.sysu.edu.cn).

Y.B.Y. and N.Y. contributed to the conception and data analyses of this work and wrote the article; Y.B.Y. conducted most of the research; J.Y. and Y.B.Y. conducted the sphingolipid detection and analysis; Y.B.Y., J.Y., and J.L. contributed to the phytohormone determination; Y.B.Y., L.Q.H., and D.K.C. contributed to investigation of the biotic resistance.

[OPEN]Articles can be viewed without a subscription.

www.plantphysiol.org/cgi/doi/10.1104/pp.19.00613

biosynthesis and signaling pathways (Yasuda et al., 2008), and promoting the storage of free SA through upregulation of the gene encoding SA glucosyl transferase and benzoic/SA carboxyl methyl transferase (Zheng et al., 2012a).

SA, an important innate immunity signal, is connected to resistance to biotrophic and hemibiotrophic pathogens (Delaney et al., 1994). Plants treated with SA or the SA analog benzothiadiazole (BTH) become more resistant to pathogens by inducing systemic acquired resistance (Görlach et al., 1996). Pretreatment with SA or BTH provokes the expression of pathogenesis-related genes upon pathogen invasion, and induces the hypersensitive response to confine the pathogen and prevent infection.

Besides playing a key role in plant defense responses, the SA pathway also affects sphingolipid metabolism. Sphingolipids are a family of complex lipids that are composed of a sphingoid long-chain base (LCB), an N-acylated fatty acid (FA), and a polar head group. Sphingolipids act not only as structural components but also signal molecules functioning in a variety of plant developmental and defense events (Pata et al., 2010; Berkey et al., 2012). Simanshu et al. (2014) showed that endogenous SA plays a role in induction of sphingolipid accumulation in *accelerated cell death11* (*acd11*). SA treatment also triggers de novo synthesis of sphingolipids (Shi et al., 2015). Moreover, defects in sphingolipid metabolism result in SA accumulation and changes in plant defense (Wang et al., 2008; Berkey et al., 2012; Bi et al., 2014). Therefore, the interaction between SA and the sphingolipid pathway is substantial and complex. In Arabidopsis guard cells, ABA activates LCBK and LCBP phosphatase activity to regulate stomatal aperture (Coursol et al., 2003; Nakagawa et al., 2012). In addition, the Arabidopsis ceramidase *At*ACER plays a role in stomatal closure (Wu et al., 2015). However, the molecular basis for the complex interplay between ABA and the sphingolipid pathway remains unclear.

Lesion-mimic mutant plants accumulate high levels of endogenous SA, and have enhanced resistance to biotic stresses (Brodersen et al., 2002; Lu et al., 2003). In contrast to most lesion-mimic mutants, the Arabidopsis ceramide kinase mutant *acd5* exhibits spontaneous cell death in its late developmental stages in a SA pathway-dependent manner (Greenberg et al., 2000). The *acd5* mutants have enhanced resistance to powdery mildew (Wang et al., 2008), but are more susceptible to *Pseudomonas syringae* and *Botrytis cinerea* than wild-type plants (Liang et al., 2003; Bi et al., 2014). Moreover, Dutilleul et al. (2015) reported that, compared with wild type, *acd5* mutants are more sensitive to ABA during germination.

In this work, we investigated the response of the *acd5* mutant to high salinity. We found that NaCl pretreatment inhibited the initiation and spread of cell death in the *acd5* mutant, partially through the antagonistic interaction between the ABA and SA pathways. Further, we found that salt treatment enhanced the resistance of Arabidopsis plants to the bacterial pathogen *P. syringae* pv *maculicola* (*Psm*) DG3, and the enhanced resistance was not due to induction of the PTI response, but to the salt-adapted physiology of the plant itself.

RESULTS

NaCl Treatment Suppresses the Cell-Death Phenotype of the *acd5* Mutant

To address the response of the *acd5* mutant to abiotic stress, we tested 22-d–old plants, a time point at which the *acd5* mutants did not show the cell-death phenotype. We induced abiotic stress by irrigating the mutant and wild-type plants with various concentrations of NaCl. The plants were irrigated once to soil capacity with NaCl solution, and then irrigated routinely with water thereafter. We found that 300-mM NaCl strongly suppressed the cell-death phenotype of the *acd5* mutant (Fig. 1, A and B), and caused no obvious damage to the wild type at the tested time point (Supplemental Fig. S1A). NaCl affected the growth of the wild type when the concentration reached 400 mM (Supplemental Fig. S1A). Therefore, we used 300-mM NaCl for the subsequent experiments.

We found that upon treatment with 300-mM NaCl, the reactive oxygen species (ROS) burst, detected by 3, 3′-diaminobenizidine (DAB) staining, and cell death, detected by trypan blue staining, were inhibited in the *acd5* mutant (Fig. 1, C and D). As shown in Supplemental Fig. S1B, NaCl treatment had no effect on the dry weight (DW) of wild-type or *acd5* mutant plants. Moreover, water and NaCl treatments did not influence the water content in tested plants (Supplemental Fig. S1B). The chlorophyll contents were similarly reduced in both wild-type and *acd5* mutants upon NaCl treatment (Supplemental Fig. S1C). These results suggested that 300-mM NaCl suppressed the cell-death phenotype of the *acd5* mutant without inhibiting plant growth. Furthermore, even after the emergence of the lesions, the NaCl-treated *acd5* mutant exhibited less cell death on the rosette leaves and stems compared to the water-treated mutant plants, indicating that NaCl inhibits the spread of cell death in *acd5* mutants (Fig. 1E).

Salt treatment can cause osmotic stress in plants (Munns and Tester, 2008); therefore, we applied a series of concentrations of mannitol to test whether the inhibitory effect of NaCl on cell death was related to osmotic stress. We found that the tested concentrations of mannitol did not inhibit the cell-death phenotype of the *acd5* mutant (Supplemental Fig. S2). Taken together, these results indicated that an appropriate concentration of NaCl could rescue the spontaneous cell-death phenotype of the *acd5* mutant, which was independent of the osmotic stress caused by salt.

NaCl Treatment Inhibites Sphingolipid Accumulation in the *acd5* Mutant

The cell-death phenotype of the *acd5* mutant is caused by accumulation of high sphingolipid levels

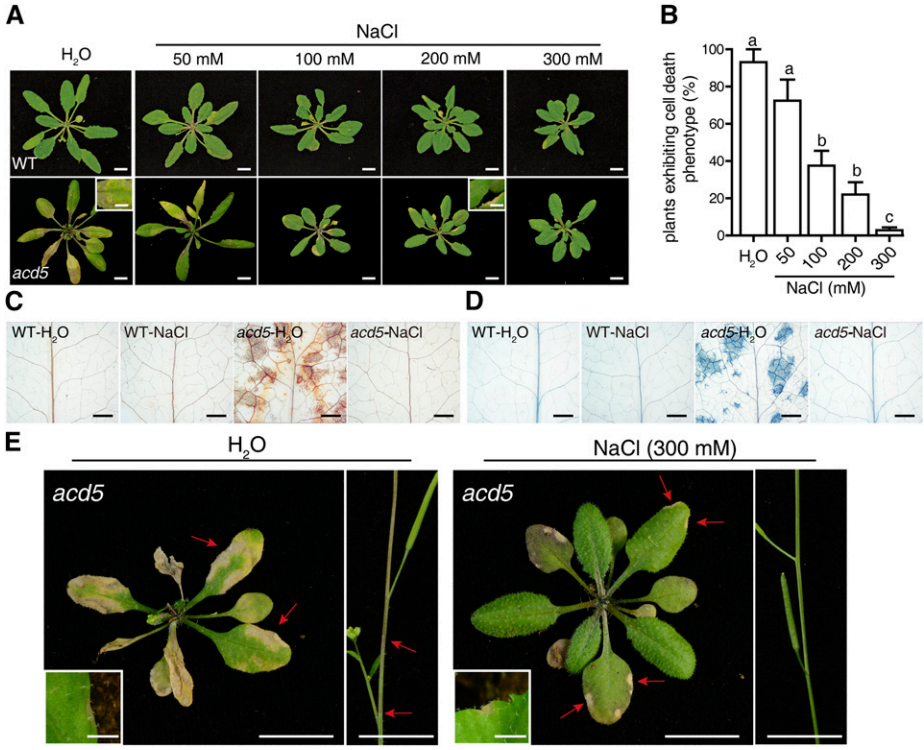

Figure 1. Phenotypes of the wild type (WT) and the *acd5* mutant after salt treatments. A–D, Three-week–old wild-type and *acd5* plants were irrigated with water or the indicated concentration of NaCl once to soil capacity and then irrigated routinely with water. A, Representative images of wild-type and *acd5* plants 21 d after NaCl treatments. Scale bars = 1 cm. The inset depicts the typical *acd5* cell death lesion; inner scale bars = 4 mm. This experiment was repeated three times with independent samples. More than 75 plants were observed for each treatment. B, Statistical analysis of the inhibitory effects of different concentrations of NaCl on the *acd5* mutant. The percentage of *acd5* plants exhibiting cell death lesions was recorded and calculated 17 d after NaCl treatment. Values are means ± SE from triplicate biological repeats ($n \geq 28$). Significant differences were determined by ANOVA post hoc test ($P < 0.05$). Note that the cell-death phenotype was barely visible in *acd5* plants under 300-mM NaCl treatment. C and D, Representative images of stained wild type and *acd5* for detection of H_2O_2 and cell death 17 d after the 300-mM NaCl treatment. Leaves were stained with DAB to detect H_2O_2 or trypan blue to detect cell death. Scale bars = 1 mm. The brown precipitate in (C) indicates DAB oxidation at the site of H_2O_2 accumulation. The blue spots in (D) indicate the dead cells visualized by trypan blue staining. At least 12 leaves were stained in each treatment. These experiments were repeated twice using independent samples. Note that no DAB or trypan blue staining was observed in the *acd5* leaves after NaCl treatment. E, After the emergence of the cell-death phenotype, 25-d–old *acd5* plants were treated with water or 300-mM NaCl. The two square inset images were recorded the phenotypes at 25 d post planting. The two main and two small rectangular images were recorded leaf and stem phenotypes 12 d after the treatment. Scale bars = 1 cm. For the inset, scale bars = 2 mm. Red arrows indicate the lesions in the *acd5* mutant. These experiments were done with three biological repeats. Note that no cell death lesions were observed in the stem after NaCl treatment (right).

(Bi et al., 2014). To check whether the sphingolipid profile was impacted by NaCl treatment, we quantified the sphingolipids in the wild-type and the *acd5* mutant by high performace liquid chromatography coupled to electrospray ionization tandem mass spectrometry after treatment with water or 300-mM NaCl. Total LCBs, glucosylceramides, and glycosylinositol phosphorylceramides (GIPCs) were not significantly different between the wild-type and *acd5* plants with or without NaCl (Fig. 2; Supplemental Fig. S3). However, the total contents of ceramides and hydroxyceramides were greatly reduced in the *acd5* mutant after NaCl treatment compared to the water-treated plants (Fig. 2A). Consistent with the total amount of sphingolipids, the accumulation of individual ceramide and hydroxyceramide species was suppressed upon NaCl treatment in the *acd5* mutant compared with the water-treated plants, especially the phytosphingosine moiety (t18:0 and t18:1) of ceramides and hydroxyceramides with long-chain FA moieties (c16:0 in ceramides and h16:0 in hydroxyceramides) and very long chain FA moieties (c24:0 and c26:0 in ceramides and h24:0 and h26:0 in hydroxyceramides; Fig. 2, B and C). These results showed that although the treatment with moderate salt concentrations did not significantly alter sphingolipid metabolism in wild type, it could remarkably suppress sphingolipid accumulation in the *acd5* mutant.

NaCl Alters the Endogenous Levels of SA and ABA

Mutants disturbing the SA pathway largely suppress the spontaneous cell-death phenotype of *acd5* (Greenberg

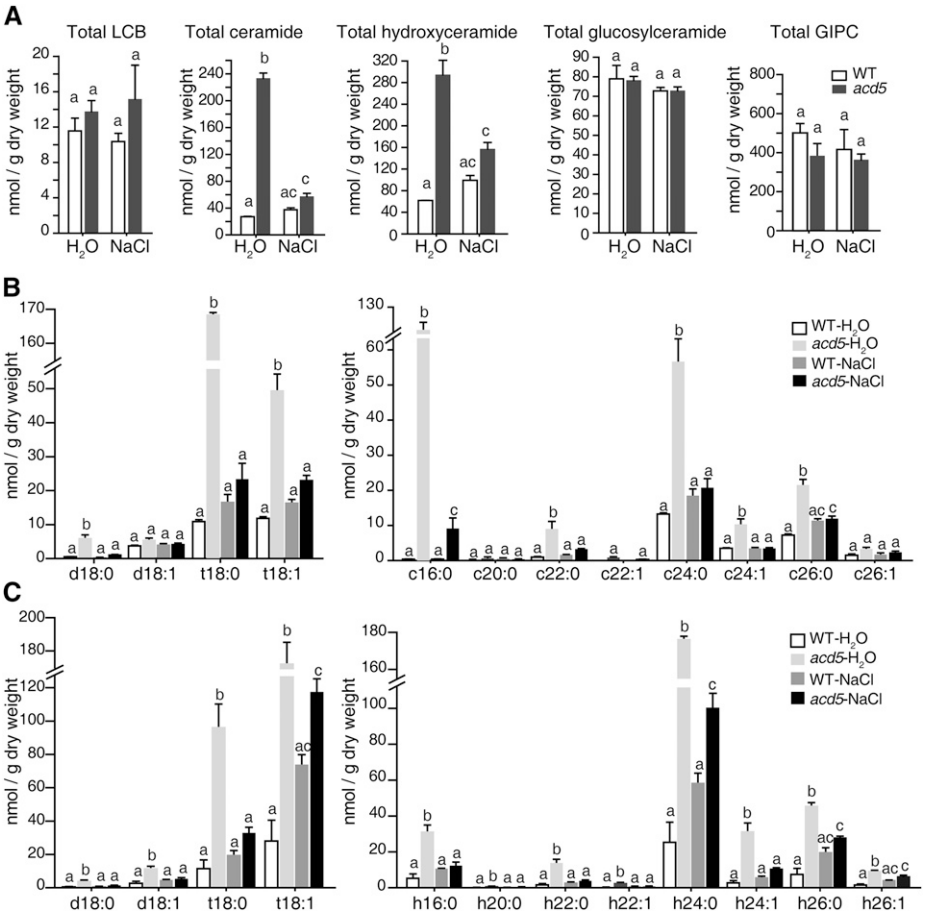

Figure 2. Sphingolipid profiles in the wild-type (WT) and *acd5* plants after NaCl treatment. Three-week–old wild-type and *acd5* plants were irrigated with water or 300-mM NaCl. Sphingolipids were extracted from rosette leaves of plants 8 d after the treatment. Values are means ± SE from triplicate technical repeats. This experiment was repeated twice using independent samples. Data sets marked with different letters indicate significant differences determined by ANOVA post hoc test ($P < 0.01$). A, Total contents of LCBs, ceramides, hydroxyceramides, glucosylceramides, and GIPCs in wild-type and *acd5* plants after NaCl treatment. B, Measurement of ceramide species with LCB moieties (left) and FA moieties (right). C, Measurement of hydroxyceramide species with LCB moieties (left) and FA moieties (right).

et al., 2000), suggesting that the SA pathway is involved in the cell-death phenotype of the *acd5* mutant. To investigate the interaction between the SA and ABA pathways during NaCl treatment, the transcript levels of ABA- and SA-related genes were measured by quantitative reverse transcription PCR (RT-qPCR). The result showed that the ABA biosynthesis gene *NCED3* was significantly downregulated (compared with the wild type under water treatment) in *acd5* at a stage when only a few cell death lesions appeared (Fig. 3A). Under the NaCl treatment, the relative expression levels of *NCED3* and the ABA downstream signaling genes *RESPONSIVE TO ABA18* (*RAB18*), *RESPONSIVE TO DEHYDRATION22* (*RD22*), and *COLD-REGULATED15A* (*COR15A*) were upregulated in the wild type and the *acd5* mutant (Fig. 3A). Consistent with previous reports (Greenberg et al., 2000), the *PATHOGENESIS-RELATED PROTEIN1* (*PR1*) expression level was high in water-treated *acd5* plants that showed spontaneous cell death lesions. By contrast, genes related to SA accumulation such as *SALICYLIC ACID INDUCTION DEFICIENT1* (*SID1*), *SID2*, *PHYTOALEXIN DEFICIENT4* (*PAD4*), and the downstream marker gene *PR1* were significantly downregulated in the *acd5* mutant under NaCl treatment compared with the *acd5*-water control (Fig. 3B). Nonetheless, as reported in Seo et al. (2008), the *PR1* expression was upregulated in wild type after NaCl treatment. The gene expression results were consistent with previous observations that NaCl treatment evokes the ABA pathway and inhibits the SA pathway (Barrero et al., 2006; Zheng et al., 2012a). These results indicated that the ABA pathway induced by NaCl treatment may suppress the cell-death phenotype of the *acd5* mutant by suppressing the SA pathway.

The endogenous levels of ABA and SA were also determined with or without NaCl treatment. As shown in Figure 3C, the amounts of ABA rapidly increased in response to NaCl treatment in the wild-type and *acd5* plants. ABA reached maximum abundance at 24 h post-treatment, and then returned to the basal level very quickly. Although the change in the amount of ABA was rapid, we also detected long-lasting expression of downstream genes 3 d post-NaCl treatment (Fig. 3A). In contrast to ABA levels, free and total SA increased gradually in the *acd5* mutant (Fig. 3, D and E; Supplemental Fig. S4), which was consistent with previous reports (Greenberg et al., 2000). As we expected, after NaCl treatment, the amount of SA in the *acd5* mutant was significantly lower than that in the water-treated mutant, and was similar to the level in the wild type (Fig. 3, D and E). These results again indicated that the induction of the ABA pathway by NaCl treatment reduced the levels of SA in the *acd5* mutant.

To verify the effects of the antagonism between the ABA and SA pathways on the phenotype of the *acd5*

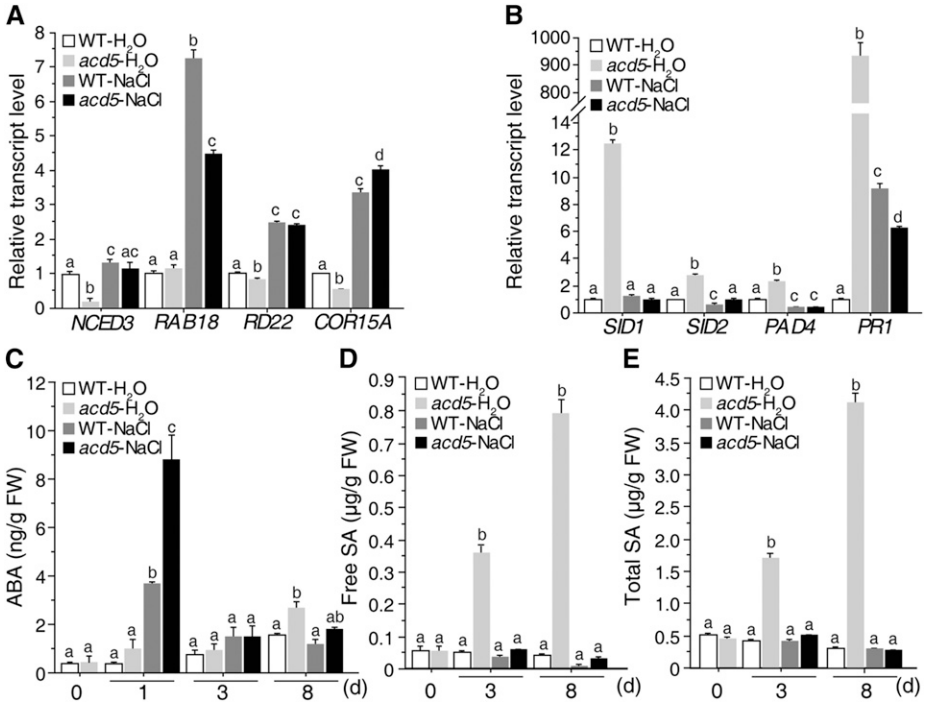

Figure 3. Influence of NaCl on ABA and SA pathways in the wild-type (WT) and *acd5* plants. Three-week–old wild-type and *acd5* plants were irrigated with water or 300-mM NaCl. The rosette leaves were collected at the indicated time points and used for RNA isolation and phytohormone extraction. These experiments were repeated at least twice using independent samples. Values are means ± SE from triplicate technical repeats. Significant differences were determined by ANOVA post hoc tests as $P < 0.05$ in (A) and (B) and $P < 0.01$ in (C–E) using different letters. A and B, Three days after NaCl treatment, the expression of the ABA biosynthesis gene *NCED3* (At3g14440), ABA downstream signaling genes *RAB18* (At5g66400), *RD22* (At5g25610), and *COR15A* (At2g42540), SA-pathway–related genes *SID1* (At4g39030), *SID2* (At1g74710), and *PAD4* (At3g52430), and the SA downstream marker gene *PR1* (At2g14610) were measured by RT-qPCR. *ACTIN2* (At3g18780) transcript levels were used as the internal control. The gene expression values presented are relative to average water-treated wild-type levels (set as "1"). C, Fluctuation of the ABA levels in wild-type and *acd5* plants after NaCl treatment. D and E, The accumulation of free SA (D) and total SA (E) in wild-type and *acd5* plants after NaCl treatment.

mutant, we tested the plants with exogenous application of ABA and the SA analog BTH. The NaCl-induced ABA level peaked at 24 h post-treatment (Fig. 3C); this suggested that 24-h post-NaCl treatment would be a good time point to test the effect of NaCl treatment on the ABA-BTH interaction. Because we did the NaCl treatment 24 h before the BTH treatment, we followed the same pattern for ABA spraying. Thus, we investigated the cell-death phenotype upon ABA or NaCl treatment, and evaluated the phenotype with ABA or NaCl plus BTH treatments. After treatment with ABA, the cell-death phenotype of the *acd5* mutant was greatly reduced by ~20% (Fig. 4, A and B). When ABA was followed by treatment with BTH, ABA suppressed BTH-induced cell death in the *acd5* mutant (Fig. 4, A and B). Therefore, pretreatment with exogenous ABA reduced the cell-death phenotype by suppressing the effects of BTH on *acd5* mutants.

We also found that NaCl antagonized the effect BTH to a greater extent than ABA did (Fig. 4, C and D). Treatment with NaCl before BTH suppressed the accumulation of ceramides and hydroxyceramides that are induced by BTH (Fig. 4E; Supplemental Fig. S5). Other sphingolipid species such as LCBs, glucosylceramides, and GIPC were not dramatically altered in response to the combined treatments (Supplemental Fig. S6). These results suggested that the inhibitory effect of NaCl on the cell-death phenotype of the *acd5* mutant may depend partially on the interaction of the ABA and SA pathways, and may suppress the SA-induced accumulation of ceramides and hydroxyceramides.

Defects in ABA Pathways Do Not Alter the Inhibition of the *acd5* Cell-Death Phenotype by NaCl

To investigate the contribution of the ABA pathway to the inhibitory effect of NaCl on the cell-death phenotype of the *acd5* mutant, we introduced the ABA signaling pathway mutations *aba-insensitive2* (*abi2-2*) and *abi4-t* (Zheng et al., 2012b; Shu et al., 2013) into the *acd5* background. The *abi2-2* mutant is insensitive to ABA and shows resistance to drought stress (Rubio et al., 2009). The *ABI4* knockout mutant *abi4-t* shows decreased seed dormancy levels and early germination, and is defective in ABA signaling (Kakizaki et al., 2009; Shu et al., 2013).

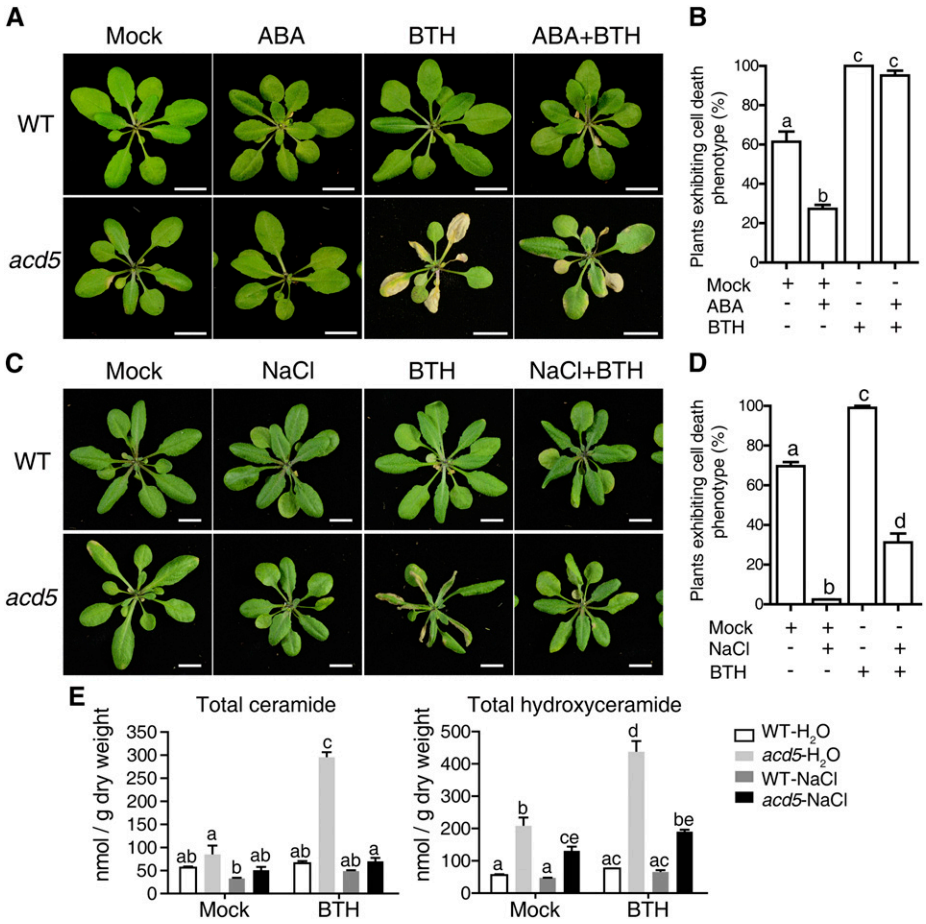

Figure 4. ABA and NaCl suppress the cell-death phenotype of the *acd5* mutant after induction by BTH. A and B, Three-week–old plants were sprayed with (+) or without (−) 400-μM ABA for 24 h, then subsequently sprayed with (+) or without (−) 300-μM BTH. Representative photos were recorded 9 d after the BTH treatment (A). Scale bars = 1 cm. B, Statistical analysis of the inhibitory effects of exogenous ABA on the *acd5* mutant cell-death phenotype after BTH induction as shown in (A). The percentage of *acd5* plants exhibiting cell death lesions in the total treated *acd5* plants was recorded. At least 24 plants were tested for each treatment. Values are means ± SE from triplicate biological repeats. Significant differences were determined by ANOVA post hoc test ($P < 0.05$). C and D, Three-week–old plants were irrigated with (+) or without (−) 300-mM NaCl for 24 h, then sprayed with (+) or without (−) 300-μM BTH. Representative photos were recorded 9 d after the BTH treatment (C). Scale bars = 1 cm. D, Statistical analysis of the inhibitory effects of NaCl on the *acd5* mutant cell-death phenotype after BTH induction as shown in (C). The percentage of *acd5* plants exhibiting cell death lesions in the total treated *acd5* plants was recorded. At least 34 plants were tested for each treatment. Values are means ± SE from triplicate biological repeats. Significant differences were determined by ANOVA post hoc test ($P < 0.05$). E, Total ceramides and hydroxyceramides in wild-type (WT) and *acd5* plants upon the combined treatments with NaCl and BTH. The rosette leaves were collected 5 d post BTH treatment. This experiment was repeated twice using independent samples. Values are means ± SE from triplicate biological repeats. Data sets marked with different letters indicate significant differences determined by ANOVA post hoc test ($P < 0.01$).

We found that without NaCl, almost 90% of the *abi4-t acd5* double mutants showed the cell-death phenotype at 26 d after germination, much earlier than the *acd5* mutants, 45% of which showed a cell-death phenotype (Supplemental Fig. S7B). In addition, the cell death lesions in the *abi4-t acd5* double mutants were much more severe than in the *acd5* mutant (Supplemental Fig. S7C). These data suggested that ABI4 may play a role in the antagonistic relationship between the ABA and SA pathways in *acd5*. However, the cell-death phenotype was delayed in the *abi2-2 acd5* double mutant, compared to the *acd5* mutant (Supplemental Fig. S7, B and C). Because of the feedback regulation of ABA metabolism, the deficiency in the ABI2 transcription factor would result in accumulation of ABA (Verslues and Bray, 2006). These results suggested that the basal ABA level in the *abi2-2 acd5* double mutant may affect the accumulation of SA and delay cell death. Taken together, these results showed that the deficiency of the ABA pathway alters the timing of cell death.

To investigate the effect of NaCl on cell death in the *abi4-t acd5* and *abi2-2 acd5* double mutants, we treated these plants with 300-mM NaCl. As shown in Figure 5, neither of these double mutants showed the cell-death

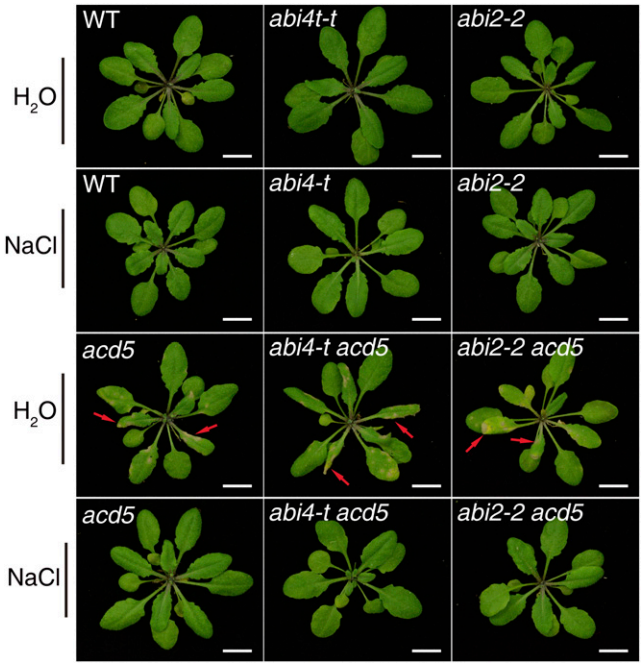

Figure 5. Effect of ABA pathway mutations on the cell-death phenotype of the *acd5* mutant after NaCl treatment. Three-week–old plants of wild-type (WT), *acd5*, *abi4-t*, *abi2-2*, and the double mutants *abi4-t acd5* and *abi2-2 acd5* were irrigated with or without 300-mM NaCl. Phenotypes were recorded 9 d after treatment. Scale bars = 1 cm. At least 16 plants per line were tested each time. Arrows indicate cell death lesions. This experiment was repeated three times using independent samples.

phenotype after NaCl treatment. Intriguingly, we also found that upon NaCl treatment, *ACD5* expression was moderately induced in both wild-type and *acd5* mutant plants (Supplemental Fig. S8), which indicated that the *ACD5* gene itself also responds to NaCl treatment. Combined with the results of the exogenous phytohormone treatments and the gene expression analysis, our data indicated that the ABA metabolism and signaling pathways were rapidly induced in response to NaCl treatment, and the exogenous application of ABA also delayed the cell-death phenotype; therefore, the inhibitory effect of NaCl on cell death in the *acd5* mutant may be partially dependent on the ABA pathway.

NaCl Treatment Enhances Resistance to Biotic Stress

SA is closely related to plant innate immunity and plays a pivotal role in the *acd5* mutant (Greenberg et al., 2000; Bi et al., 2014). To understand whether the NaCl treatment affects the response to biotic stress, Arabidopsis plants were pretreated with NaCl and then inoculated with the bacterial pathogen *Psm* DG3, which was derived from *Psm* strain ES4326 (Liang et al., 2003). As shown in Figure 6A, wild-type and *acd5* plants pretreated with NaCl showed less-severe pathogenic lesions than the water-treated controls. The trypan blue staining also showed less cell death in the NaCl-treated wild-type and *acd5* plants (Fig. 6B).

To verify the level of resistance of the NaCl-treated plants, the abundance of pathogenic bacteria in the leaves was measured by the leaf-disc method. The bacterial abundance was greatly suppressed in the NaCl pretreated wild-type and *acd5* plants (Fig. 6C). These results indicated that a 24-h pretreatment with 300-mM NaCl enhanced the plant's resistance to biotic stress.

Because NaCl treatment suppressed the SA level in *acd5* (Fig. 3, D and E) and enhanced plant resistance to bacterial infection (Fig. 6), we wondered whether the SA pathway was induced in response to the pathogen and

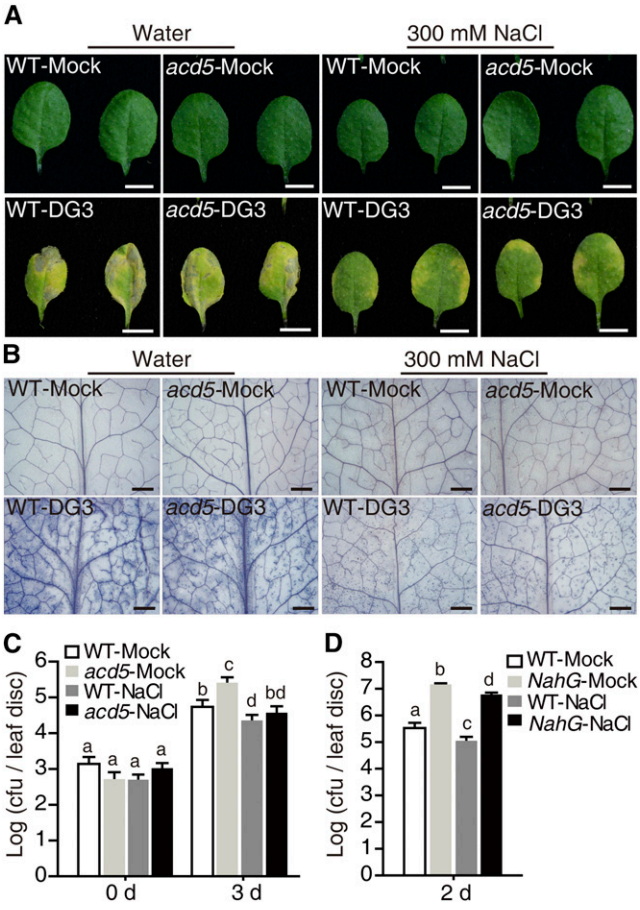

Figure 6. NaCl treatment enhanced plant resistance to bacterial infection. Three-week–old wild-type (WT) and *acd5* plants were treated with or without 300-mM NaCl. After 24 h of treatment, leaves were infiltrated with the virulent *Psm* DG3 at OD_{600} = 0.0005. The experiment was repeated three times by using independent samples. A, Representative leaves 4 d after *Psm* DG3 inoculation. At least 32 plants were infiltrated for each case. Scale bars = 5 mm. B, Representative microscopic images of leaves post *Psm* DG3 infection. At 2 d post inoculation, at least nine infected leaves were detached and stained with trypan blue to observe cell death. Scale bars = 1 mm. C and D, Leaf discs from 3-week–old wild type, *acd5*, and *NahG* plants were harvested for quantification of bacterial growth at 3 d post infiltration (C) or 2 d post infiltration (D). Bacterial growth was measured as colony-forming units (cfu)/disc of leaf tissue. Values are means ± SE from at least six biological replicates. Significant differences were determined by ANOVA post hoc tests ($P < 0.05$) using different letters.

contributed to the enhancement of biotic resistance by NaCl treatment. Therefore, we used transgenic *NahG* plants, which express a bacterial SA-hydroxylase and effectively degrade SA. Compared to mock treatment, pretreatment with NaCl also prevented bacterial growth in the *NahG* plants. The propagation of pathogenic bacteria was significantly higher in the NaCl-treated *NahG* plants than in the NaCl-treated wild type (Fig. 6D). These results suggested that pretreatment with NaCl enhanced the plant's resistance to pathogenic agents, which is partially dependent on the SA pathway.

Pathogen-Associated Molecular PTI Is Not Enhanced in the NaCl-Treated Plants

Singh et al. (2014) demonstrated that abiotic stresses could prime the PTI response to enhance the plant's resistance to biotic stress. To verify whether the enhanced resistance to *Psm* DG3 in this study was dependent on the PTI response, we tested the *P. syringae* pv tomato strain DC3000 (*Pst* DC3000) *hrcC* mutant (lacking a functional type-III secretion system), which does not induce PTI, and flagellin epitope flg22, which does induce PTI. To measure the response, callose deposition was examined and ROS were measured in the control and NaCl pretreated plants (Singh et al., 2014). As shown in Figure 7, A–D, after pretreatment with NaCl, no dramatic increase in callose deposition was measured after induction by *Pst* DC3000 *hrcC* or flg22 in either the wild-type or the *acd5* plants. In addition, the flg22-induced ROS burst showed no obvious difference between the water- and NaCl-pretreated plants (Fig. 7E). The results indicated that pretreatment with NaCl does not prime the PTI response to resist pathogen infection. Further, the PTI marker gene *FLG22-*

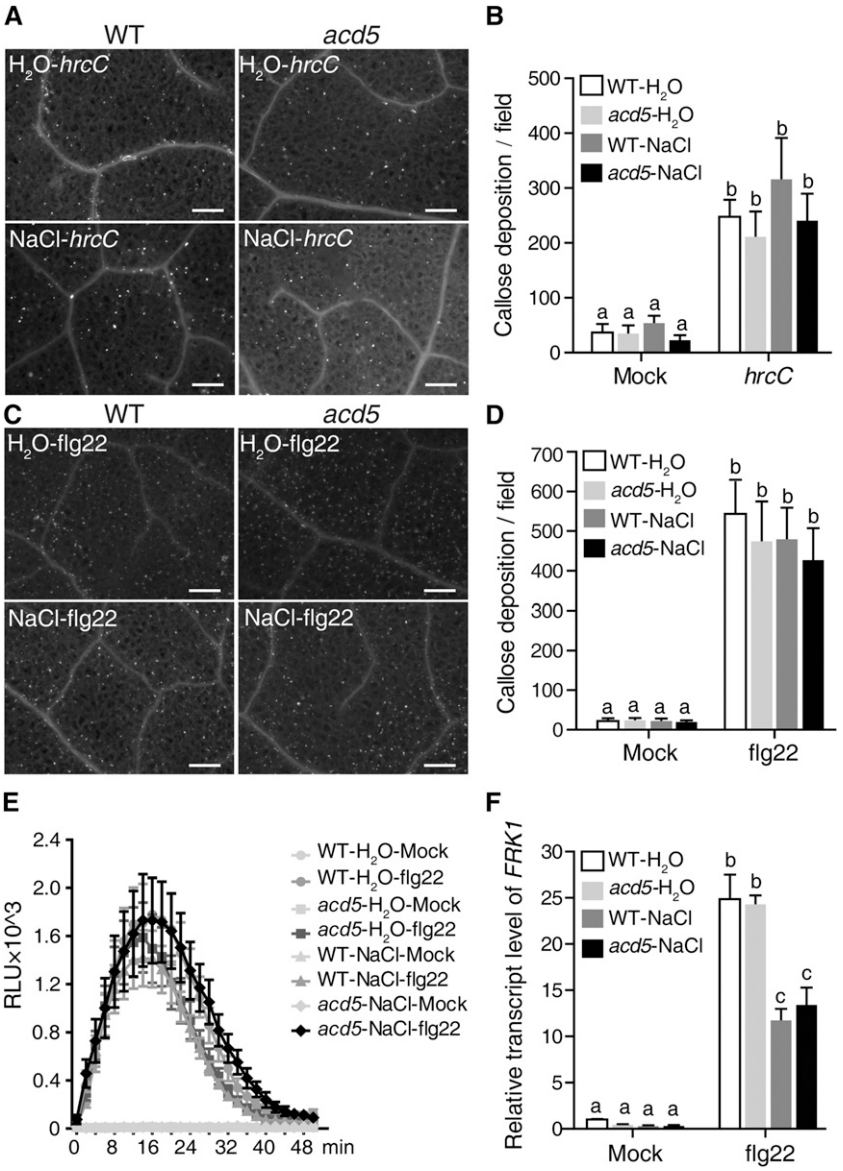

Figure 7. Effect of NaCl pretreatment on the pattern-triggered immune response. Three-week–old wild-type (WT) and *acd5* plants were irrigated with or without 300-mM NaCl. A to D, At 24 h after irrigation with or without 300-mM NaCl, the plants were inoculated with the *Pst* DC3000 mutant *hrcC* (OD_{600} 0.01) for 24 h (A and B) or 100 nM of the biologically active epitope of bacterial flagellin flg22 for 12 h (C and D). Scale bars = 200 μm (A and C). Images were photographed by fluorescence microscopy and the callose deposition (the white spots) was calculated by the software ImageJ (National Institutes of Health). Values in (B) and (D) = means ± SE from at least eight biological repeats. These experiments were repeated three times. Significant differences were determined by ANOVA post hoc tests ($P < 0.05$) using different letters. E, ROS production induced by flg22. At 24 h after the water or NaCl treatment, leaf discs (diameter = 0.5 mm) from third to fifth leaves were treated with 100-nM flg22 or mock (distilled water). ROS were recorded by a luminol-based assay, presented as relative light units (RLUs). Data represent means ± SE from eight biological replicates. Significant differences were determined by ANOVA post hoc tests ($P < 0.05$) using different letters. This experiment was repeated three times using independent samples. F, The relative transcript level of *FRK1* (At2g19190) after flg22 induction. At 24 h after the water or 300-mM NaCl treatment, 100-nM flg22 was infiltrated into the third to fifth leaves. The RNA samples were collected 3-h post infiltration. Data represent means ± SE from triplicate technical replicates. Significant differences were determined by ANOVA post hoc tests ($P < 0.05$) using different letters. This experiment was repeated twice using independent samples.

INDUCED RECEPTOR-LIKE KINASE1 (*FRK1*) was detected after the combined treatment of NaCl and flg22. Intriguingly, the flg22-induced transcription of *FRK1* (Singh et al., 2014) was significantly higher in the water-treated control plants than in the NaCl-treated plants (Fig. 7F). These results suggested that the NaCl pretreatment does not prime the plant PTI response against biotic stress.

Based on our results, we hypothesized that after the NaCl pretreatment, the microenvironment of the plant's intercellular space was unfavorable for colonization by the pathogenic bacteria. Pro positively regulates plant resistance to biotic stresses by adjusting the osmotic balance and the redox status of cells (Phang et al., 2010; Ben Rejeb et al., 2015). We measured the Pro content after the NaCl treatment. As shown in Figure 8A, after NaCl treatment, both the wild-type and *acd5* plants accumulated >15× higher levels of free Pro when compared with the water-treated control. This result suggested that in the acclimation to saline conditions, the accumulation of Pro aided the plants in adjusting their metabolism.

NaCl causes cell death in plants due to ion disequilibrium (Huh et al., 2002), and salt-sensitive plants have increased electrolyte leakage because of the impact on cell membrane integrity (Verslues et al., 2006). Therefore, we measured the relative electrolyte leakage in the wild type and the *acd5* mutant after NaCl treatment. The electrolyte leakage was greatly increased in the NaCl-treated plants compared with the water-treated plants (Fig. 8B). However, no trypan blue staining was observed in the rosette leaves of the NaCl-treated plants (Fig. 1D), suggesting that the increased electrolyte leakage did not result from dead cells induced by the saline condition. Electrolytes accumulate in the apoplastic spaces of the plant leaf tissue, which may change the physicochemical property of the intercellular space where the pathogens colonize; therefore, we measured the effect of NaCl on bacterial growth in vitro. As shown in Figure 8C, when we increased the NaCl concentration in the *Psm* DG3 liquid culture medium, the proliferation of bacteria was greatly reduced; this was in line with the bacterial growth tendency in vivo, which was suppressed in plants by pretreatment with NaCl (Fig. 6, C and D). These results indicated that the resistance of the plants to *Psm* DG3 might be related to the accumulation of electrolytes in the intercellular space after NaCl treatment, which may weaken the ability of the bacteria to colonize the plant.

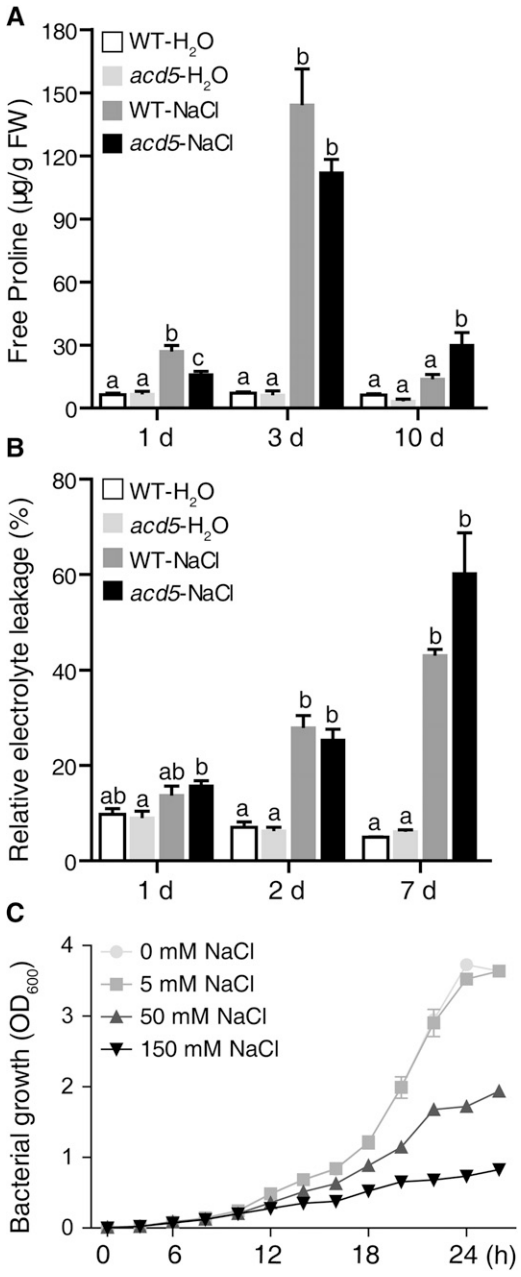

Figure 8. Effects of NaCl on Pro, electrolyte leakage of plants, and *Psm* DG3 growth. Three-week–old plants were irrigated with 300-mM NaCl or water. Rosette leaves were harvested to extract free Pro or to detect relative electrolyte leakage at the indicated time points. These experiments were repeated twice using independent samples. A, The accumulation of free L-Pro in wild-type (WT) and *acd5* plants. Data represent means ± SE from triplicate biological repeats. B, The electrolyte leakage of wild-type and *acd5* plants was detected at the indicated time points. Data represent means ± SE from triplicate biological repeats. Significant differences were determined by ANOVA post hoc tests ($P < 0.01$) using different letters. C, Effect of NaCl on the growth of *Psm* DG3 in vitro. Different concentrations of NaCl were added to the bacterial liquid culture medium. The abundance of *Psm* DG3 was measured by a spectrophotometer at OD_{600} at the indicated time points. Data represent means ± SE from four biological repeats.

DISCUSSION

In this study, we demonstrated that pretreatment with NaCl inhibits the cell-death phenotype of the *acd5* mutant, which is deficient in ceramide kinase. The inhibition of cell death and the spread of the lesions was partially dependent on the antagonistic interaction between the ABA and SA pathways, and subsequently, the accumulation of sphingolipids in the *acd5* mutant

was also suppressed. Further, NaCl pretreatment enhanced the plant's resistance to biotic stress by suppressing the growth of *Psm* DG3 pathogenic bacteria.

The *acd5* plants accumulate high levels of sphingolipids late in development, especially ceramides and hydroxyceramides (Bi et al., 2014). Additionally, the *acd5* mutants accumulate high levels of SA after lesions appear (Greenberg et al., 2000; Liang et al., 2003; Fig. 3). The activation of the SA pathway might be pivotal for sphingolipid accumulation and the cell-death phenotype of the *acd5* mutant. Similar to *acd5 nahG* (Greenberg et al., 2000), NaCl treatment inhibited the spontaneous cell-death phenotype of *acd5* in the late developmental stage in a manner independent of the osmotic effect of salt stress.

Previous studies have shown that NaCl treatment induces ABA biosynthesis and signaling, which has an antagonistic interaction with SA (Yasuda et al., 2008; Zheng et al., 2012a; Ding et al., 2016). In our study, in the *acd5* mutant treated with NaCl, the ABA and SA pathways showed the same antagonistic effect. Under the NaCl treatment, the ABA pathway was rapidly induced, whereas the SA pathway was moderately downregulated compared with the water-treated control plants. We noticed that without NaCl treatment, the expression of *NCED3* was downregulated in *acd5* mutants compared to wild type (Fig. 3A). We detected the level of expression 3 d after the treatments, when the *acd5*-water plants already exhibited a few cell death lesions, and at this time point SA had significantly accumulated in the *acd5*-water plants (Fig. 3, D and E). Overexpression of *NCED3* can result in higher ABA accumulation and suppress the SA pathway (Fan et al., 2009; Oide et al., 2013). *NCED3* could also be induced by NaCl treatment (Fig. 3A). These results suggest that *NCED3* may be a key player in the NaCl–ABA-mediated inhibition of cell-death in the *acd5* mutant.

In the water-treated *acd5* mutant, the SA level gradually increased, consistent with previous studies (Greenberg et al., 2000; Bi et al., 2014). The accumulation of sphingolipids is tightly related to the SA pathway (Simanshu et al., 2014; Shi et al., 2015). After BTH treatment, high amounts of sphingolipids accumulated (Fig. 4E) in *acd5* mutants and the NaCl pretreatment could suppress the effect of BTH on sphingolipid accumulation in *acd5* mutants (Fig. 4E). Taking these observations together, we speculated that the reduced sphingolipid contents in the NaCl-treated *acd5* mutant might result from impairment of the SA pathway.

Treatments with exogenous ABA and the SA analog BTH were conducted to examine the metabolism and signaling of endogenous hormones (Yasuda et al., 2008). Although ABA treatment did not inhibit the late developmental stage cell-death phenotype of the *acd5* mutant, it substantially delayed cell death and minimized the induction of cell death in the *acd5* mutant by BTH. These results suggested that the ABA pathway has an antagonistic interaction with the SA pathway. However, when the NaCl and BTH treatments were combined, NaCl suppressed the effect of BTH much more effectively than ABA did. Therefore, we speculated that NaCl may induce other ABA-independent pathways (Barrero et al., 2006; Munns and Tester, 2008) to suppress the cell-death phenotype.

The introduction of the *abi* mutations *abi2-2* and *abi4-t* into the *acd5* background affected the timing of emergence of the cell-death phenotype (Supplemental Fig. S7), indicating that a partially interrupted ABA pathway also affects the *acd5* phenotype. We inferred that these ABA pathway mutations altered endogenous SA metabolism and signaling pathways in the *acd5* mutant. The cell-death phenotype of the *abi4-t acd5* double mutant was much more severe than in the *acd5* single mutant (Supplemental Fig. S7). ABI4, a member of the AP2/ERF family, plays multiple roles in plant development and response to environmental stresses (Wind et al., 2013). Shkolnik-Inbar et al. (2013) showed that under salt stress, the *abi4* mutant accumulates less Na^+ and more Pro in shoots than wild type. The ion disequilibrium induced by salt stress can result in cell death (Huh et al., 2002). We speculate that the development of cell death in *acd5* may have a relationship with ion balance. In the *abi4 acd5* double mutants, this produced an early cell-death phenotype (Supplemental Fig. S7B), which might result from a more severe ion disequilibrium compared with the parent line. In the *abi2-2 acd5* double mutant, the occurrence of cell death lesions is delayed (Supplemental Fig. S7B). This could be due to feedback regulation of ABA metabolism by ABI2, and results in an increased ABA level in *abi2-2* mutants (Verslues and Bray, 2006; Rubio et al., 2009). In addition, we treated the *abi4-t acd5* and *abi2-2 acd5* double mutants with 300-mM NaCl to check whether NaCl suppresses the cell-death phenotype. Unexpectedly, none of the mutants displayed the cell-death phenotype after NaCl treatment (Fig. 5). These results suggest that the ABA pathway may play only a minor role in the inhibitory effect of NaCl on the cell-death phenotype of the *acd5* mutant, and further study is needed to fully understand the mechanism behind the inhibitory role of NaCl.

In plants infected with *Psm* DG3 without NaCl pretreatment, the *acd5* mutant was much more susceptible than wild type (Fig. 6C), consistent with previous results (Greenberg et al., 2000). In addition, NaCl pretreatment enhanced disease resistance of the wild-type plants and the *acd5* mutant (Fig. 6, A–C). Dutilleul et al. (2015) reported that cold stress alters the *ACD5* transcript level and ceramide kinase activity in the *acd5* mutant. Thus, we determined the *ACD5* expression upon NaCl treatment. The results showed that under water treatment, the *acd5* mutant showed higher *ACD5* expression than wild type, which might result from feedback regulation because of the dysfunction of ACD5 ceramide kinase activity (Supplemental Fig. S8). Intriguingly, upon NaCl treatment, *ACD5* expression was slightly increased in wild type (Supplemental Fig. S8). These results suggested that *ACD5* may play an important role both in plant–pathogen interactions and NaCl responses.

Singh et al. (2014) demonstrated that after treatment with NaCl, an enhanced PTI response increased plants'

resistance to pathogen attack. Therefore, we investigated the PTI response of the plants in our study. Unexpectedly, we found no significant differences in the callose deposition and ROS production induced by the *hrcC* mutant or flg22 between the NaCl-treated plants and the water-treated ones in the wild type and the *acd5* mutant (Fig. 7). *FRK1* encodes a receptor-like kinase and is widely used as a marker gene for flg22-induced PTI responses (Singh et al., 2014); after the flg22 treatment, *FRK1* was expressed at a much lower level when the plants were pretreated with NaCl as compared with the plants treated with water (Fig. 7F). The flg22-induced *FRK1* expression can be affected by defects in the SA pathway (Yi et al., 2014), and the SA pathway was suppressed by NaCl pretreatment (Fig. 3, D and E), even in conditions that induce SA (Fig. 4C) and upon pathogen infection (Fig. 6D). Therefore, we speculated that the downregulated expression of *FRK1* in NaCl-treated plants after flg22 induction might result from suppression of the SA pathway. These results suggest that the NaCl pretreatment did not result in enhanced PTI responses upon pathogen infection.

When confronted with abiotic stresses, plants undergo a reprogramming phase while adapting to the new growth conditions, which involves an increase in the level of Pro (Phang et al., 2010; Ben Rejeb et al., 2015). In our study, Pro accumulated to a greater extent in the NaCl-treated plants compared to the water-treated plants at 3 d post treatment. Electrolytes also accumulated in the NaCl-treated plants, but no cell death was observed (Fig. 1D); therefore, we speculated that the electrolytes accumulated from the intercellular fluids might result from plant adaptive responses to a saline environment (Munns and Tester, 2008). Thus, the relative electrolyte leakage in Figure 8B indicated there was a higher ionic strength in intercellular space of NaCl-treated plants compared with the water-treated ones. Because we already showed that *Psm* DG3 growth is stunted in NaCl-pretreated plants in Figure 6, C and D, and NaCl can suppress the growth of *Psm* DG3 in KB medium (Fig. 8C), the conductivity changes in the intercellular space may also affect *Psm* DG3 proliferation.

In summary, we found that NaCl pretreatment inhibits the cell-death phenotype and the accumulation of sphingolipids in the *acd5* mutant, which may be partially dependent on the antagonism between ABA and SA. Additionally, pretreatment with NaCl enhanced disease resistance in the wild-type and the *acd5* plants, which was not due to the PTI response, but to changes in the physiology of the plant to adapt to the saline environment. However, further investigation is needed to better understand the mechanisms behind these phenotypes.

MATERIALS AND METHODS

Plant Materials and Growth Conditions

Arabidopsis (*Arabidopsis thaliana*) ecotype Col-0, as wild-type and *acd5* null mutant plants, was grown on soil as described in Bi et al. (2014). The T-DNA insertion mutants of *abi2-2* (SALK_015166C) and *abi4-t* (SALK_080095) were obtained from the Arabidopsis Biological Resource Center (http://www.arabidopsis.org/abrc/). The *abi2-2 acd5* and *abi4-t acd5* double mutants were generated by crossing the indicated T-DNA mutant into the *acd5* background. The homozygous F_3 plants were used in this study.

Salt Treatments and Chlorophyll Content Determination

Soil-grown plants were irrigated with water, NaCl, or mannitol solutions once to soil capacity and then subsequently irrigated with water as required. Phenotypes and plant materials were recorded and harvested. The fresh weight (FW) was recorded at the time when the rosette leaves were collected. After incubation at 100°C for 15 min to deactivate enzyme activity in the tissue, the materials were kept in a 60°C hot-air oven to obtain constant DW. The water content was calculated as: water content (%) = $(FW - DW)/FW \times 100$. Chlorophyll content was measured as described in Wu et al. (2015).

Histochemical Staining

The ROS were detected by DAB staining, cell death was detected by trypan blue staining, and callose depositions were detected by aniline blue staining as described in Bi et al. (2014). Briefly, plant leaves were submerged in the trypan blue solution containing 2.5 mg of trypan blue (cat. no. T6146; Sigma-Aldrich) per mL, 25% (v/v) lactic acid, 25% (v/v) water-saturated phenol, 25% (v/v) glycerol, and 25% (v/v) distilled water. Then, the leaves were heated in boiling water for 2 min, cooled at room temperature, and decolorized in a chloral hydrate solution (2.5 g of chloral hydrate dissolved in 1 mL of distilled water) for at least 10 h. Samples were equilibrated with 50% (v/v) glycerol for microscopy.

Sphingolipid Assay

Samples for sphingolipid analysis were prepared as described in Bi et al. (2014), Wu et al. (2015), and Li et al. (2016).

Gene Expression Analysis by RT-qPCR

The differences in gene expression between the control and NaCl treatments were compared using real-time Taq Man-PCR techniques (Applied Biosystems). Total RNA was isolated using the E.Z.N.A. plant RNA Kit (cat. no. R6827-01; Omega Bio-tek) according to the manufacturer's instructions. For each sample, 1 μg of RNA was reverse-transcribed into cDNA using the PrimeScript RT reagent kit with genomic DNA Eraser (Takara). A total of 1 μL of diluted cDNA samples (1:20) was mixed with 5 mL 2 × SYBR Premix Ex Taq II (Takara) and 0.4 μL of gene-specific primers in 384-well plates (Roche) and then quantitatively analyzed by a LightCycler480 Real-Time PCR System (Roche). Three technical replicates were performed for each template and primer combination. *ACTIN2* was analyzed as the internal reference gene to normalize values for transcript abundance. The $2^{-\triangle\triangle CT}$ method (Livak and Schmittgen, 2001) was used to calculate the relative expression level of the target genes. The primers for amplification are listed in Supplemental Table S1.

Phytohormone Treatment and Measurement

For the BTH and ABA treatments, three-week–old plants grown in soil were sprayed with 400 μM of ABA or ethanol (mock). After 24 h, 300-μM BTH or 0.3% [v/v] acetone (mock) was applied.

SA contents were extracted and measured by high-performance liquid chromatography analysis as described by Wang et al. (2011) with minor modifications. Briefly, 100 mg of plant material was ground to a fine powder with liquid nitrogen and extracted with 1 mL of 90% (v/v) methanol containing with 500 ng of o-anisic acid (lot no. L740L01; J&K) as an internal control. After transferring the methanol fraction into a new microcentrifuge tube, the residual fraction was resuspended with 750 μL of absolute methanol by vortexing and then the methanol fraction was collected once again. The two methanol fractions were combined and distributed into two microcentrifuge tubes equally, then dried under nitrogen. The pellet was dissolved by adding 500 μL of 100-mM sodium acetate at pH 5.5. To half of the duplicated samples, 10 μL of 40-mg/mL β-glucosidase (lot no. BCBB5805V; Sigma-Aldrich) was added to digest glucosyl-conjugated SA. For all the samples, 50 μL of 50% [v/v] TCA was added and the samples were centrifuged at 10,000*g* for 10 min. The supernatant was extracted with 1.25 mL of extraction buffer (ethylacetate:cyclopentane:2-propanol 100:99:1, v/v/v). The top phase was collected and dried under

nitrogen. The residual fraction was resuspended in 500 μL of 55% (v/v) methanol by vortexing and centrifuged. The supernatant was subjected to a Dionex UltiMate 3000 Fluorescence Detector System (Thermo Fisher Scientific) using a Luna C18 column (250 × 4.6 mm, 5 μm; Phenomenex).

ABA was extracted and measured as described in Yuan et al. (2017). Briefly, leaf tissues were collected and frozen in liquid nitrogen. The powdered samples (50 mg) were added into microcentrifuge tubes containing 500 μL of extraction buffer (concentrated HCl:isopropanol:ddH_2O 1:1,000:500, v/v/v) with 10 ng of D_6-ABA as internal standard. The samples were gently agitated for 30 min at 4°C, then 1 mL of CH_2Cl_2 was added and the samples were agitated for another 30 min. After centrifugation, the lower phase was collected and dried under nitrogen. The pellets were dissolved in 100 μL 60% (v/v) methanol and analyzed with a model no. UFLC-XR (Shimadzu) coupled with a quadrupole TripleTOF 5600+ System (AB SCIEX) using a Luna C18 column (150 × 2.1 mm, 2.6 μm; Phenomenex).

Pseudomonas syringae Infection and Bacterial Growth Assay

At 1 d after NaCl treatment, third-to-fifth leaves of three-week–old plants were inoculated with *P. syringae* pv *maculicola* strain DG3 at OD_{600} 0.0005- or 10-mM $MgSO_4$ (mock) as described in Li et al. (2016). For the bacterial growth assay, at least six independent leaf discs were collected at each time point to determine the population of bacteria as colony forming units. After 24 h of NaCl treatment, third-to-fifth leaves of three-week–old plants were inoculated with *P. syringae* pv tomato strain DC3000 *hrcC* at an OD_{600} of 0.01. After inoculation for 24 h, callose deposition was detected by aniline blue staining.

Detection of Flg22-Induced ROS

The flg22-induced ROS signal was monitored using a GloMax 96 Microplate Luminometer (Promega) by measuring the relative light units of luminescence (Wu et al., 2015). Leaf discs (diameter = 5 mm) were incubated in distilled water in 96-well flat-bottomed white plates overnight in the dark at room temperature. The next day, the distilled water was substituted with a solution containing 34-μg/mL luminol (A8511; Sigma-Aldrich), 20-μg/mL peroxidase (P6782; Sigma-Aldrich), and 100-nM flg22 (synthesized by Sangon Biotech).

Pro Detection

Free Pro content in leaf tissues was extracted according to a method described in Ben Rejeb et al. (2015). Briefly, plant leaf tissues were collected and ground into fine powder. The samples were suspended in 5 mL of 3% (w/v) sulphosalicylic acid and kept in boiling water for 10 min, then cooled to room temperature. The supernatant was transferred into a new tube and reacted with glacial acetic acid and ninhydrin reagent for 40 min in boiling water. After cooling to room temperature, the samples were extracted with toluene. The top phase was collected to detect the A_{520}. Pro concentration was calculated from the absorbance of a series of Pro standards assayed in an identical way.

Relative Electrolyte Leakage

The electrolyte leakage was determined as described in Yuan et al. (2017). Briefly, the third-to-sixth rosette leaves of at least three plants were collected. After adding deionized water, the samples were gently agitated at room temperature for 1 h and the conductivity of the solution was measured. Total electrolyte strength was determined after heating the solution in a 100°C water bath for 10 min and cooling to room temperature. The relative electrolyte leakage was calculated by comparing leaked ionic strength with the corresponding total ionic strength.

Statistical Analyses

Data are presented as means ± SE. Significant differences were determined by ANOVA post hoc tests in conjunction with Fisher's protected least significant difference test ($P < 0.05$, $P < 0.01$) using different letters. The number of biological replicates or technical repeats is given in the figure legends.

Accession Numbers

NCED3 (At3g14440), *RAB18* (At5g66400), *RD22* (At5g25610), *COR15A* (At2g42540), *SID1* (At4g39030), *SID2* (At1g74710), *PAD4* (At3g52430), *PR1* (At2g14610), *ACD5* (AT5G51290), *FRK1* (AT2G19190), *ACTIN2* (At3g18780).

Supplemental Data

The following supplemental materials are available.

Supplemental Figure S1. Inhibitory effect of NaCl on the cell-death phenotype of the *acd5* mutant.

Supplemental Figure S2. Effect of mannitol treatments on the cell-death phenotype of the *acd5* mutant.

Supplemental Figure S3. The sphingolipid contents in wild-type and *acd5* plants after NaCl treatment.

Supplemental Figure S4. SA detection at 24 h after NaCl treatment.

Supplemental Figure S5. The ceramide and hydroxyceramide species in wild-type and *acd5* plants after the combined NaCl and BTH treatment.

Supplemental Figure S6. The glucosylceramide, LCB, and GIPC species in wild-type and *acd5* plants after the combined NaCl and BTH treatment.

Supplemental Figure S7. The influence of ABA pathway mutants on the cell-death phenotype of the *acd5* mutant.

Supplemental Figure S8. *ACD5* expression upon salt treatment.

Supplemental Table S1. Primers for qPCR used in this study.

ACKNOWLEDGMENTS

We thank Prof. Xiao Shi for kindly providing us the internal standard for ABA quantification, d_6-ABA. We thank the Arabidopsis Biological Resource Center for the mutant seeds.

Received May 22, 2019; accepted June 14, 2019; published June 26, 2019.

LITERATURE CITED

Baena-González E, Rolland F, Thevelein JM, Sheen J (2007) A central integrator of transcription networks in plant stress and energy signalling. Nature **448:** 938–942

Barrero JM, Rodríguez PL, Quesada V, Piqueras P, Ponce MR, Micol JL (2006) Both abscisic acid (ABA)-dependent and ABA-independent pathways govern the induction of NCED3, AAO3 and ABA1 in response to salt stress. Plant Cell Environ **29:** 2000–2008

Ben Rejeb K, Lefebvre-De Vos D, Le Disquet I, Leprince AS, Bordenave M, Maldiney R, Jdey A, Abdelly C, Savouré A (2015) Hydrogen peroxide produced by NADPH oxidases increases proline accumulation during salt or mannitol stress in *Arabidopsis thaliana*. New Phytol **208:** 1138–1148

Berkey R, Bendigeri D, Xiao S (2012) Sphingolipids and plant defense/disease: The "death" connection and beyond. Front Plant Sci **3:** 68

Bi FC, Liu Z, Wu JX, Liang H, Xi XL, Fang C, Sun TJ, Yin J, Dai GY, Rong C, et al (2014) Loss of ceramide kinase in *Arabidopsis* impairs defenses and promotes ceramide accumulation and mitochondrial H_2O_2 bursts. Plant Cell **26:** 3449–3467

Brodersen P, Petersen M, Pike HM, Olszak B, Skov S, Odum N, Jørgensen LB, Brown RE, Mundy J (2002) Knockout of *Arabidopsis accelerated-cell-death11* encoding a sphingosine transfer protein causes activation of programmed cell death and defense. Genes Dev **16:** 490–502

Coursol S, Fan LM, Le Stunff H, Spiegel S, Gilroy S, Assmann SM (2003) Sphingolipid signalling in Arabidopsis guard cells involves heterotrimeric G proteins. Nature **423:** 651–654

Delaney TP, Uknes S, Vernooij B, Friedrich L, Weymann K, Negrotto D, Gaffney T, Gut-Rella M, Kessmann H, Ward E, et al (1994) A central role of salicylic acid in plant disease resistance. Science **266:** 1247–1250

Ding Y, Dommel M, Mou Z (2016) Abscisic acid promotes proteasome-mediated degradation of the transcription coactivator NPR1 in *Arabidopsis thaliana*. Plant J **86:** 20–34

Dutilleul C, Chavarria H, Rézé N, Sotta B, Baudouin E, Guillas I (2015) Evidence for ACD5 ceramide kinase activity involvement in Arabidopsis response to cold stress. Plant Cell Environ **38:** 2688–2697

Fan J, Hill L, Crooks C, Doerner P, Lamb C (2009) Abscisic acid has a key role in modulating diverse plant-pathogen interactions. Plant Physiol **150:** 1750–1761

Görlach J, Volrath S, Knauf-Beiter G, Hengy G, Beckhove U, Kogel KH, Oostendorp M, Staub T, Ward E, Kessmann H, et al (1996) Benzothiadiazole, a novel class of inducers of systemic acquired resistance, activates gene expression and disease resistance in wheat. Plant Cell **8:** 629–643

Greenberg JT, Silverman FP, Liang H (2000) Uncoupling salicylic acid-dependent cell death and defense-related responses from disease resistance in the *Arabidopsis* mutant *acd5*. Genetics **156:** 341–350

Huh GH, Damsz B, Matsumoto TK, Reddy MP, Rus AM, Ibeas JI, Narasimhan ML, Bressan RA, Hasegawa PM (2002) Salt causes ion disequilibrium-induced programmed cell death in yeast and plants. Plant J **29:** 649–659

Iuchi S, Kobayashi M, Taji T, Naramoto M, Seki M, Kato T, Tabata S, Kakubari Y, Yamaguchi-Shinozaki K, Shinozaki K (2001) Regulation of drought tolerance by gene manipulation of 9-cis-epoxycarotenoid dioxygenase, a key enzyme in abscisic acid biosynthesis in *Arabidopsis*. Plant J **27:** 325–333

Kakizaki T, Matsumura H, Nakayama K, Che FS, Terauchi R, Inaba T (2009) Coordination of plastid protein import and nuclear gene expression by plastid-to-nucleus retrograde signaling. Plant Physiol **151:** 1339–1353

Li J, Yin J, Rong C, Li KE, Wu JX, Huang LQ, Zeng HY, Sahu SK, Yao N (2016) Orosomucoid proteins interact with the small subunit of serine palmitoyltransferase and contribute to sphingolipid homeostasis and stress responses in *Arabidopsis*. Plant Cell **28:** 3038–3051

Liang H, Yao N, Song JT, Luo S, Lu H, Greenberg JT (2003) Ceramides modulate programmed cell death in plants. Genes Dev **17:** 2636–2641

Livak KJ, Schmittgen TD (2001) Analysis of relative gene expression data using real-time quantitative PCR and the $2^{(-\triangle\triangle CT)}$ method. Methods **25:** 402–408

Lu H, Rate DN, Song JT, Greenberg JT (2003) ACD6, a novel ankyrin protein, is a regulator and an effector of salicylic acid signaling in the Arabidopsis defense response. Plant Cell **15:** 2408–2420

Melotto M, Underwood W, Koczan J, Nomura K, He SY (2006) Plant stomata function in innate immunity against bacterial invasion. Cell **126:** 969–980

Munns R, Tester M (2008) Mechanisms of salinity tolerance. Annu Rev Plant Biol **59:** 651–681

Nakagawa N, Kato M, Takahashi Y, Shimazaki K, Tamura K, Tokuji Y, Kihara A, Imai H (2012) Degradation of long-chain base 1-phosphate (LCBP) in Arabidopsis: Functional characterization of LCBP phosphatase involved in the dehydration stress response. J Plant Res **125:** 439–449

Nambara E, Marion-Poll A (2005) Abscisic acid biosynthesis and catabolism. Annu Rev Plant Biol **56:** 165–185

Oide S, Bejai S, Staal J, Guan N, Kaliff M, Dixelius C (2013) A novel role of PR2 in abscisic acid (ABA) mediated, pathogen-induced callose deposition in *Arabidopsis thaliana*. New Phytol **200:** 1187–1199

Pata MO, Hannun YA, Ng CK (2010) Plant sphingolipids: Decoding the enigma of the Sphinx. New Phytol **185:** 611–630

Phang JM, Liu W, Zabirnyk O (2010) Proline metabolism and microenvironmental stress. Annu Rev Nutr **30:** 441–463

Raghavendra AS, Gonugunta VK, Christmann A, Grill E (2010) ABA perception and signalling. Trends Plant Sci **15:** 395–401

Rubio S, Rodrigues A, Saez A, Dizon MB, Galle A, Kim TH, Santiago J, Flexas J, Schroeder JI, Rodriguez PL (2009) Triple loss of function of protein phosphatases type 2C leads to partial constitutive response to endogenous abscisic acid. Plant Physiol **150:** 1345–1355

Seo PJ, Lee AK, Xiang F, Park CM (2008) Molecular and functional profiling of Arabidopsis pathogenesis-related genes: Insights into their roles in salt response of seed germination. Plant Cell Physiol **49:** 334–344

Shi C, Yin J, Liu Z, Wu JX, Zhao Q, Ren J, Yao N (2015) A systematic simulation of the effect of salicylic acid on sphingolipid metabolism. Front Plant Sci **6:** 186

Shkolnik-Inbar D, Adler G, Bar-Zvi D (2013) ABI4 downregulates expression of the sodium transporter HKT1;1 in Arabidopsis roots and affects salt tolerance. Plant J **73:** 993–1005

Shu K, Zhang H, Wang S, Chen M, Wu Y, Tang S, Liu C, Feng Y, Cao X, Xie Q (2013) ABI4 regulates primary seed dormancy by regulating the biogenesis of abscisic acid and gibberellins in Arabidopsis. PLoS Genet **9:** e1003577

Simanshu DK, Zhai X, Munch D, Hofius D, Markham JE, Bielawski J, Bielawska A, Malinina L, Molotkovsky JG, Mundy JW, et al (2014) ARABIDOPSIS ACCELERATED CELL DEATH 11, ACD11, is a ceramide-1-phosphate transfer protein and intermediary regulator of phytoceramide levels. Cell Reports **6:** 388–399

Singh P, Yekondi S, Chen PW, Tsai CH, Yu CW, Wu K, Zimmerli L (2014) Environmental history modulates Arabidopsis pattern-triggered immunity in a HISTONE ACETYLTRANSFERASE1-dependent manner. Plant Cell **26:** 2676–2688

Verslues PE, Bray EA (2006) Role of abscisic acid (ABA) and *Arabidopsis thaliana* ABA-insensitive loci in low water potential-induced ABA and proline accumulation. J Exp Bot **57:** 201–212

Verslues PE, Agarwal M, Katiyar-Agarwal S, Zhu J, Zhu JK (2006) Methods and concepts in quantifying resistance to drought, salt and freezing, abiotic stresses that affect plant water status. Plant J **45:** 523–539

Wang GF, Seabolt S, Hamdoun S, Ng G, Park J, Lu H (2011) Multiple roles of WIN3 in regulating disease resistance, cell death, and flowering time in *Arabidopsis*. Plant Physiol **156:** 1508–1519

Wang W, Yang X, Tangchaiburana S, Ndeh R, Markham JE, Tsegaye Y, Dunn TM, Wang GL, Bellizzi M, Parsons JF, et al (2008) An inositolphosphorylceramide synthase is involved in regulation of plant programmed cell death associated with defense in *Arabidopsis*. Plant Cell **20:** 3163–3179

Wind JJ, Peviani A, Snel B, Hanson J, Smeekens SC (2013) ABI4: Versatile activator and repressor. Trends Plant Sci **18:** 125–132

Wu JX, Li J, Liu Z, Yin J, Chang ZY, Rong C, Wu JL, Bi FC, Yao N (2015) The Arabidopsis ceramidase AtACER functions in disease resistance and salt tolerance. Plant J **81:** 767–780

Yasuda M, Ishikawa A, Jikumaru Y, Seki M, Umezawa T, Asami T, Maruyama-Nakashita A, Kudo T, Shinozaki K, Yoshida S, et al (2008) Antagonistic interaction between systemic acquired resistance and the abscisic acid-mediated abiotic stress response in Arabidopsis. Plant Cell **20:** 1678–1692

Yi SY, Shirasu K, Moon JS, Lee SG, Kwon SY (2014) The activated SA and JA signaling pathways have an influence on flg22-triggered oxidative burst and callose deposition. PLoS One **9:** e88951

Yuan LB, Dai YS, Xie LJ, Yu LJ, Zhou Y, Lai YX, Yang YC, Xu L, Chen QF, Xiao S (2017) Jasmonate regulates plant responses to postsubmergence reoxygenation through transcriptional activation of antioxidant synthesis. Plant Physiol **173:** 1864–1880

Zheng XY, Spivey NW, Zeng W, Liu PP, Fu ZQ, Klessig DF, He SY, Dong X (2012a) Coronatine promotes *Pseudomonas syringae* virulence in plants by activating a signaling cascade that inhibits salicylic acid accumulation. Cell Host Microbe **11:** 587–596

Zheng Y, Schumaker KS, Guo Y (2012b) Sumoylation of transcription factor MYB30 by the small ubiquitin-like modifier E3 ligase SIZ1 mediates abscisic acid response in *Arabidopsis thaliana*. Proc Natl Acad Sci USA **109:** 12822–12827